J. Fluid Mech. (1979), *vol.* 95, *part* 1, *pp.* 199–208
Printed in Great Britain

Experimental study of the instabilities of waves obliquely incident on a beach

By R. T. GUZA AND D. C. CHAPMAN

Shore Processes Laboratory, Scripps Institution of Oceanography,
La Jolla, California 92093

(Received 21 September 1978 and in revised form 20 November 1978)

Monochromatic waves obliquely incident on a plane beach, and strongly reflected there, are unstable to perturbations by edge waves. Theory suggests the possible width of the resonant edge wave frequency band. Experiments on beaches with absorbers at both ends show that the excited waves have frequencies at the centre of the band, as predicted by Guza & Bowen (1975). Advection by mean longshore currents must be taken into account. If reflectors are placed at the beach ends, the additional boundary conditions apparently lead to resonances scattered across the resonant band.

1. Introduction

A monochromatic unidirectional wave train incident from deep water on a uniformly sloping beach (and strongly reflected there) can exchange energy with edge-wave perturbations in a nonlinear resonant triad. For the case of normally incident waves, Guza & Davis (1974) showed that the most rapidly growing edge-wave perturbation consists of two progressive edge waves (each of half the frequency of the incident wave) but travelling in opposite directions resulting in a standing subharmonic edge wave. Guza & Inman (1975) observed this pattern in laboratory experiments and investigated the importance of the spacing of reflective barriers at the beach ends. They found the spacing to be crucial (especially for long edge waves) since it imposes boundary conditions which restrict the possible edge wave modes, and also guarantees a certain symmetry between up and down coast propagating waves. The edge waves formed beach cusps when sand tracers were placed on the concrete laboratory beach. Huntley & Bowen (1978) have recently shown field data which suggest that subharmonic edge waves form cusps.

The final amplitude of the edge waves is limited by the third-order effects of finite amplitude detuning and radiation of edge wave energy to the far field (Guza & Bowen 1976*a*). The edge wave equilibrium amplitude, based on shallow water equations, is

$$\epsilon_e \simeq \epsilon_i^{\frac{1}{2}}, \tag{1}$$

where $\epsilon = \hat{a}\hat{\omega}^2/g \tan^2\beta$, $\hat{a}$ and $\hat{\omega}$ are the amplitude and angular frequency, respectively, for the incident (i) or edge (e) waves, g is gravitational acceleration, and β is the beach slope. Rockliff (1978), from a more systematic approach, developed the case of subharmonic edge waves generated by normally incident waves between reflective barriers and found finite amplitude effects very similar to those of Guza & Bowen (1976*a*).

0022-1120/79/4327-7680 $02.00

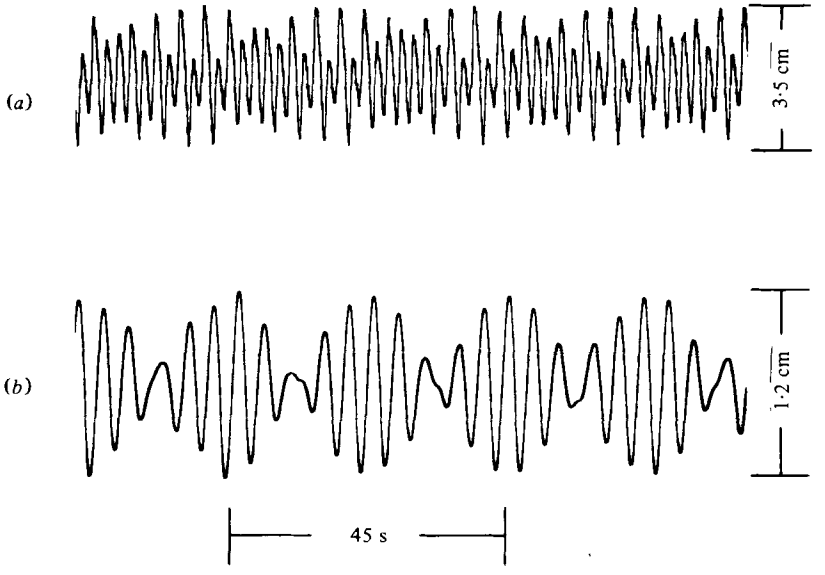

FIGURE 1. Typical strip chart record showing (*a*) the unfiltered sea surface elevation, and (*b*) the edge wave signal (incident waves having been filtered out) showing the amplitude modulation described in the text.

Minzoni & Whitham (1977) independently reached a similar conclusion without resorting to shallow water approximations. Rockliff (1978) presented the detailed algebra for the higher-order synchronous edge wave resonance suggested by Guza & Inman (1975). Laboratory experiments (Guza & Inman 1975) qualitatively agree with (1); in that the edge-wave amplitude at the shoreline is larger than that of the incident wave. The subharmonic resonance does not occur with weakly reflected incident waves, possibly because of increased dissipation associated with incident wave breaking (Guza & Bowen 1976*b*). The work discussed above suggests that edge-wave generation by monochromatic, strongly reflected, normally incident waves is well understood.

The extension of theory to non-normally incident waves is simple (Guza & Bowen 1975; hereinafter referred to as GB75) and shows that most rapidly growing edge wave perturbations consist of two progressive, zero mode, edge waves propagating in opposite directions, but having slightly different frequencies. This results in a pseudo-subharmonic standing wave pattern which slowly drifts in the longshore direction. The theoretical shoreline configuration is given by (for the resonance having the most rapid initial growth rate),

$$\hat{\eta} = 2\hat{a}_e \sin\left(\frac{\hat{\omega}_i}{2}\hat{t} + \Delta k\hat{y}\right)\cos\left(\hat{k}_e\hat{y} + \frac{\hat{\omega}_i}{2}\gamma t\right), \tag{2}$$

where $\hat{\eta}$ is sea surface elevation, $\hat{k}_e = \hat{\omega}_i^2/4g\beta$, Δk is the difference in longshore wavenumbers of the two edge waves, $\gamma = \tan\beta\sin\alpha_\infty \ll 1$, α_∞ is the deep water angle of incidence, $\hat{t}$ is time, and $\hat{y}$ is the longshore direction. Terms of $O(\gamma^2)$ have been neglected. At a fixed $\hat{y}$ location, we should observe a pattern of subharmonic ($\frac{1}{2}\hat{\omega}_i$) motion modulated at the beat frequency $\frac{1}{2}\hat{\omega}_i\gamma$. Equivalently, a given edge wave antinode should appear to slowly drift downcoast with speed $2g\beta\gamma/\omega_i$. Experiments (described later) immediately revealed that the modulation frequency (or drift rate) was not that

predicted by theory. Figure 1(*b*), for example, shows a measured modulation period of 46 s compared to a theoretical value of 88 s.

Two possible causes of the discrepancy were examined. First, since the modulation frequency depends on the frequencies of the excited edge waves, the condition that the excited edge waves be those with the maximum initial growth rate, as was implicitly assumed in GB75, was relaxed. This suggests a possible width of the resonant edge-wave frequency band. Second, the effects on the edge-wave pattern of advection by a mean longshore current due to the obliquely incident waves was considered. Advection was found to be the most important effect.

2. Theory

(*a*) *Departures from exact resonance*

We will consider the growth of the lowest mode, almost subharmonic edge waves forced by obliquely incident waves, with the frequency of the edge waves slightly different from exact resonant coupling. We first introduce the dimensionless variables (circumflex referring to dimensional variables) by the definitions:

$$(x,y) = \frac{\hat{\omega}_i^2}{g\tan\beta}(\hat{x},\hat{y}), \quad t = \hat{\omega}_i\hat{t}, \quad \Phi = \frac{\hat{\omega}_i}{\hat{a}_1 g}\hat{\Phi}. \tag{3}$$

We assume edge-wave perturbations of the form

$$\Phi_e = \sum_{j=1,2} a_j \phi_j(x)\sin(k_j y + \omega_j t + \theta_j), \tag{4}$$

where

$$\phi_j = \omega_j^{-1}\exp[-|k_j|x].$$

Both amplitudes, a_j, and phases, θ_j, can be slow functions of time. We assume that the resonance conditions hold:

$$\omega_1 + \omega_2 = 1 \tag{5a}$$

and

$$k_1 + k_2 = \gamma; \tag{5b}$$

the angular frequencies, however, can each differ from those of exact resonance by a small constant $\Delta\omega$,

$$\omega_1 = \tfrac{1}{2}(1+\gamma) + \Delta\omega$$

and

$$\omega_2 = \tfrac{1}{2}(1-\gamma) - \Delta\omega. \tag{6}$$

Edge waves with frequencies given by (6) do not exactly satisfy the linear dispersion relation for zero mode edge waves, and hence will have reduced initial resonant growth rates. These edge waves will, however, have altered modulation frequencies, $\hat{\omega}_1[\frac{1}{2}\gamma + \Delta\omega]$ instead of $\frac{1}{2}\hat{\omega}_1\gamma$.

Proceeding as did GB75 (however, allowing θ_j to vary in t) we obtain the following equations for amplitudes and phases by eliminating secular terms arising from the nonlinear interaction of edge and incident waves:

$$\frac{da_1}{dt} = \epsilon_1\delta_1 a_2 \sin(\theta_1+\theta_2), \tag{7a}$$

$$\frac{d\theta_1}{dt} = 2\epsilon_1\delta_1\frac{a_2}{a_1}\cos(\theta_1+\theta_2) - \frac{\Delta\omega(1+\gamma)}{\omega_1}, \tag{7b}$$

$$\frac{da_2}{dt} = \epsilon_1 \delta_2 a_1 \sin(\theta_1 + \theta_2) \tag{7c}$$

and

$$\frac{d\theta_2}{dt} = 2\epsilon_1 \delta_2 \frac{a_1}{a_2} \cos(\theta_1 + \theta_2) + \frac{\Delta\omega(1-\gamma)}{\omega_2}, \tag{7d}$$

where

$$\delta_1 = \frac{|k_1|}{\omega_2} \int_0^\infty \phi_1 I_2 \, dx, \quad \delta_2 = \frac{|k_2|}{\omega_1} \int_0^\infty \phi_2 I_1 \, dx$$

and

$$I_j = \frac{\partial \phi_j}{\partial x} \frac{\partial \phi_i}{\partial x} (\omega_j - 1) + k_j \gamma \phi_j \phi_i (1 - \omega_j) + \frac{\omega_j \phi_j}{2} \left[\frac{\partial^2 \phi_j}{\partial x^2} - \gamma^2 \phi_i \right] - \frac{\phi_i}{2} \left[\frac{\partial^2 \phi_j}{\partial x^2} - k_j^2 \phi_j \right].$$

Numerical integration shows that $\delta_1 = \delta_2(1 + O(\gamma))$, the $O(\gamma)$ term resulting from differences in the wavenumber–frequency ratios (not from the integrals). For simplicity and since $\gamma \ll 1$, we will assume $\delta_1 \simeq \delta_2 \simeq \delta$. Numerical integration of equations (7*a*) and (7*c*) then shows that if $a_1(0) \neq a_2(0)$, they will rapidly approach some common value. Thus, we can assume $a_1 = a_2 = a_e$ and rewrite equations (7) as:

$$\frac{da_e}{dt} = \epsilon_1 \delta a_e \sin(\theta_1 + \theta_2), \tag{8a}$$

$$\frac{d}{dt}(\theta_1 + \theta_2) = 4\epsilon_1 \delta \cos(\theta_1 + \theta_2) - \Delta\omega \left(\frac{1+\gamma}{\omega_1} - \frac{1-\gamma}{\omega_2} \right). \tag{8b}$$

For general initial phases $(\theta_1 + \theta_2)$, if the right-hand side of (8*b*) ever becomes identically zero, then $(\theta_1 + \theta_2)$ is constant, and a_e grows exponentially. Only initial phases such that, at $t = 0$, $d(\theta_1 + \theta_2)/dt = 0$ and $\sin(\theta_1 + \theta_2) < 0$, do not lead to exponential growth. If $\theta_1 + \theta_2$ never becomes constant, then a_e oscillates about its initial small value $a_e(0)$. Thus, exponential growth occurs when

$$\cos(\theta_1 + \theta_2) = \frac{\Delta\omega}{4\epsilon_i \delta} \left(\frac{1+\gamma}{\omega_1} - \frac{1-\gamma}{\omega_2} \right), \tag{9}$$

which places an upper limit on $\Delta\omega$, since $|\cos(\theta_1 + \theta_2)| < 1$. However, as $\Delta\omega$ approaches this limit, the growth rate approaches zero (since as $\cos(\theta_1 + \theta_2) \to 1$, $\sin(\theta_1 + \theta_2) \to 0$) and we might realistically expect a narrower resonant band than given by solving (9) for $\Delta\omega_{\max}$ with $\cos(\theta_1 + \theta_2) = \pm 1$. We therefore numerically integrated (8), solving for a_e, arbitrarily selecting a small value of $a_e(0) = \hat{a}_e(0)/\hat{a}_i(0) = 0{\cdot}1$. Equation (1) gives a non-dimensional equilibrium edge wave amplitude (when higher order terms limit growth) of $a_e = 4/\epsilon_i^{\frac{1}{2}}$. Integration of (8), which does not include the higher order terms, was stopped when a_e reached this value, and the elapsed time taken as a characteristic time to reach equilibrium. The characteristic times were effectively independent of initial phase choice and γ, and are shown in figure 2. The very large times to reach equilibrium at the largest values of $\Delta\omega$ for each ϵ_i make these formally resonant cases inapplicable to our laboratory experiments where no cases of very slow growth were observed. We therefore chose the bandwidth limits shown by circles on figure 2; these $\Delta\omega$ have altered modulation times compared to $\Delta\omega = 0$, but basically unchanged

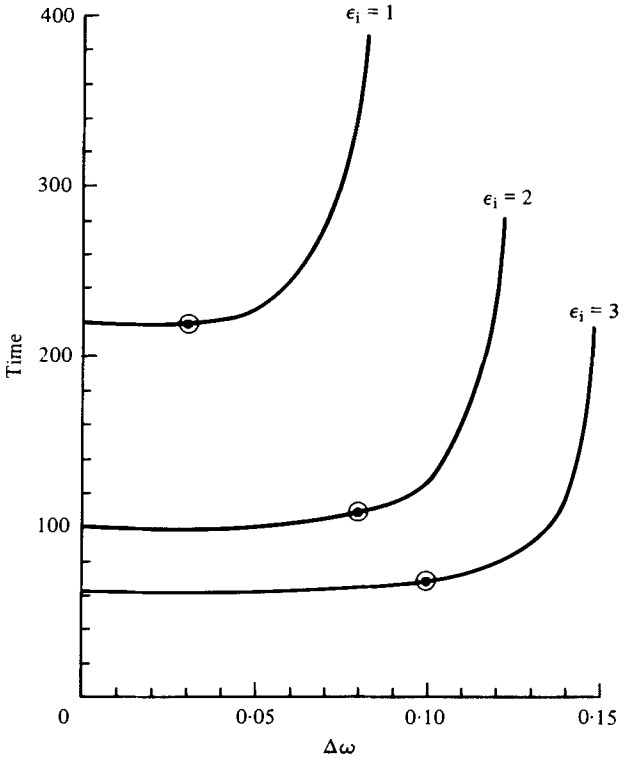

FIGURE 2. Non-dimensional time for edge waves to reach equilibrium for various values of $\Delta\omega$, ϵ_i. Circles show the approximate upper bound on $\Delta\omega$ as discussed in the text.

growth rates. Slightly different choices of bandwidth result from different choices of $a_e(0)$, but our modified bandwidths are already only qualitative. The sea surface elevation at the shoreline can be written (in dimensional form):

$$\hat{\eta} = 2\hat{a}_e \sin\left(\frac{\hat{\omega}_i}{2}\hat{t} + \Delta k\hat{y}\right)\cos\left(\hat{k}_e\hat{y} + \frac{\hat{\omega}_i}{2}\gamma\hat{t} + \hat{\omega}_i\Delta\omega\hat{t}\right). \tag{10}$$

We see that the only effect of $\Delta\omega$ is to change the angular beat frequency by an amount $\hat{\omega}_i\Delta\omega$ from that of the exact resonance case.

(*b*) *Advection by longshore current*

A uniform steady current of velocity U will introduce a beating into a standing wave (observed at a fixed point) of frequency

$$\hat{\omega}_B^u = \hat{k}_e U. \tag{11}$$

Using the edge-wave dispersion relation ($\hat{\omega}_e^2 = g\beta\hat{k}_e$) and non-dimensionalizing,

$$\omega_B^u = \frac{\hat{\omega}_i U}{4g\beta}. \tag{12}$$

By observing the beating for a given situation, we can estimate the beat frequency of the waves alone by

$$\omega_B^e = \omega_B^o - \omega_B^u \tag{13}$$

where ω_B^o is the observed beat frequency. This can be compared to that predicted by GB75 of

$$\omega_B^p = \tfrac{1}{2}\gamma \tag{14}$$

from which a value of $\Delta\omega$ can be estimated as

$$\Delta\omega = \omega_B^o - \omega_B^p. \tag{15}$$

We note that although a longshore shear current will change the 'angle' of the incident waves propagating over it, the longshore wavenumber k_l will be conserved (Kenyon 1971). Since the fundamental definition of γ depends only on k_l and $\tan\beta$, the current will not alter γ and the theoretically predicted modulation frequency (14). The on–offshore shape of the incident standing wave profile, however, will be slightly altered by a shear current resulting in a small change in the coupling coefficient δ and the theoretically predicted bandwidths (figure 2). We neglect this effect.

3. Experiments

Experiments were performed in the Hydraulics Laboratory at Scripps Institution of Oceanography. Incident waves were generated over the entire basin length (15 m) by a hydraulically controlled, wedge shaped plunger type paddle in water of constant, 51 cm, depth. The beach slope, β, was 6°. Wide absorbers were placed at the ends of the beach to simulate an infinitely long beach. The entire side walls were also lined with dissipators to reduce multiple reflexions on the incident wave. These were evidently effective because any re-reflexions of the obliquely incident wave would not be incident at $\pm\alpha_\infty$ and any additional excited edge waves would have a modulation frequency different from that of the primary edge waves. Multiple modulation frequencies were never observed.

Sea surface elevation was measured with a resistance wire. Electronic filters were used to remove the nearly subharmonic edge wave signal from that of the incident waves (figure 1). Modulation times were estimated from the strip charts by averaging ten consecutive modulation periods. Individual modulation periods could be estimated within $\pm$ 1 s and remained virtually constant throughout each average.

The run-up due to the incident wave alone was measured to give an estimate of ϵ_l. Since $\beta \sim 2a_l/R$, where R is the total swash excursion,

$$\epsilon_l \simeq \frac{R}{2}\frac{\hat{\omega}_l^2}{g\beta}. \tag{16}$$

The equivalent angle of deep water incidence, α_∞, was calculated from the conservation of longshore wavenumber:

$$k_\infty \sin\alpha_\infty = k_l \sin\alpha_p,$$

where $k_\infty = \hat{\omega}_l^2/g$ is the deep water longshore wavenumber, k_l is the incident longshore wavenumber at the paddle, and α_p is the angle between the paddle and the undisturbed shoreline. Using the linear dispersion relation for surface gravity waves,

$$\sin\alpha_\infty = \frac{\sin\alpha_p}{\tanh k_l h}, \tag{17}$$

where h is the water depth at the paddle (51 cm).

The effectiveness of the absorbers in preventing edge wave reflexion was verified in two ways. First, the measured decay time of the edge waves, after the wavemaker was turned off, was about the time for a progressive edge wave to travel the length of the beach. This indicates minimal side wall reflexion. Secondly, observation near an absorber showed little subharmonic amplitude modulation (unlike figure 1 observed in the basin centre) indicating that only a single progressive edge wave was present there. This also indicates low side wall reflectivity.

We note in passing that when the edge waves reach their final equilibrium amplitude, there are necessarily longshore variations in edge-wave amplitude since no energy propagates away from the absorbers. This is of no consequence here, however, since the preceding analysis for amplitude growth in time can be converted to longshore distance co-ordinates using

$$\delta/\delta t = C_g \delta/\delta y.$$

Thus, the theory which predicts long times to reach equilibrium amplitudes, equivalently predicts long non-dimensional distances and our basic conclusions about the effects of $\Delta\omega$ and currents are unaltered.

Subharmonic modulation times were measured at different locations along the beach, and showed no spatial dependence. Extensive measurements were made with different deep water angles of incidence ($-0{\cdot}16°$, $11{\cdot}1°$, $26{\cdot}6°$) and an incident wave frequency of 0·48 Hz.

The mean longshore current was crudely measured using dye and slightly positively buoyant spheres. Measurements were complicated by the large swash motions associated with the edge waves. Also, the mean current was strongest at the shoreline, rapidly decaying offshore. The mean current was estimated by placing the spheres in the swash, and averaging the resulting longshore velocities together. The longshore current was averaged over an offshore distance of about 0·6 m, which is about $0{\cdot}25\lambda_y$ with λ_y the edge-wave wavelength. This is not an inappropriate averaging distance since the edge wave decays exponentially offshore, and is 0·2 of its shoreline value when $X = \frac{1}{4}\lambda_y$. The measurements of mean longshore current showed increasing scatter for increasing currents. For the worst cases, the standard deviation was the size of the mean. For the best case, $\alpha_\infty = -0{\cdot}16°$, dye was observed to not advect at all, so the mean current was accurately taken as zero.

4. Results

While the theoretical development assumes that the incident waves are strongly reflected at the beach, all of the measurements reported here are cases in which $\epsilon_1 \geqslant 1$ which indicates that some wave breaking occurred (Guza & Bowen 1976*b*). Table 1 shows typical values of ϵ_1, U, ω_B^o, ω_B^u. For the smallest incident waves, the longshore current is also a minimum and it continues to increase with increasing ϵ_1, even though the edge-wave amplitudes are maximum for $\epsilon_1 \approx 2$. In fact, a large current was observed even after the incident waves became so large as to cleanly break and prevent all edge-wave growth. This indicates that the longshore current was not the result of an edge-wave–edge-wave interaction, but was associated with the incident wave breaking. This is also supported by the large relative magnitude of the longshore current velocity.

ϵ_i	U (cm s^{-1})	ω_B^u (10^{-2})	ω_B^o (10^{-2})
1·19	0·73	0·53	1·30
1·59	0·96	0·70	1·53
1·77	1·05	0·77	1·65
2·00	1·06	0·77	1·74
2·21	1·07	0·78	1·93

TABLE 1. Typical values of ϵ_i, U, ω_B^u, ω_B^o for $\alpha_\infty = 11{\cdot}1°$. Longshore current accounts for over 40% of ω_B^o in all cases.

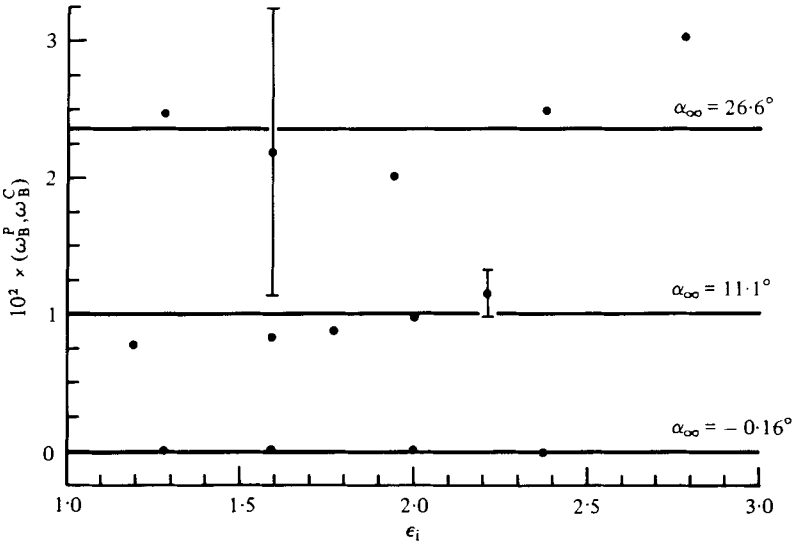

FIGURE 3. Predicted non-dimensional beat frequency (ω_B^p, solid lines) and corresponding experimental beat frequencies (ω_B^c, dots) for different deepwater incident angles (α_∞) and ϵ_i. The vertical lines show estimates of typical error due to velocity measurements.

A comparison of the calculated modulation frequency, $\omega_B^c = \omega_B^o - \omega_B^u$, and the predicted value, ω_B^p, is shown in figure 3 for various values of ϵ_i. The vertical error bars indicate typical variations in the measurements resulting from the inaccuracy of U as mentioned earlier. For $\alpha_\infty = -0{\cdot}16°$, the observed U was too small to estimate, and $\omega_B^c \simeq \omega_B^o \simeq 0$ in all cases. The general agreement is good which indicates that most of the difference between theory and observation is accountable as longshore current effects. The dependence of observed modulation frequency on incident wave amplitude simply reflects the increased longshore current.

Figure 4 shows the estimated values of $\Delta\omega$ [see equation (15)] along with the approximate theoretical bandwidth discussed in § 2. We see that $\Delta\omega$ always falls within the resonant frequency band. In fact, the data suggests $\Delta\omega = 0$, the resonance with the most rapid initial growth rate. This is also a very likely initial perturbation since it is a free wave.

The edge-wave equilibrium amplitudes ($\epsilon_i < 2$) agreed with (1), derived for normally incident waves. This is expected since the coupling coefficients and other parameters are weak functions of γ. The resonance was suppressed by excessive breaking of the

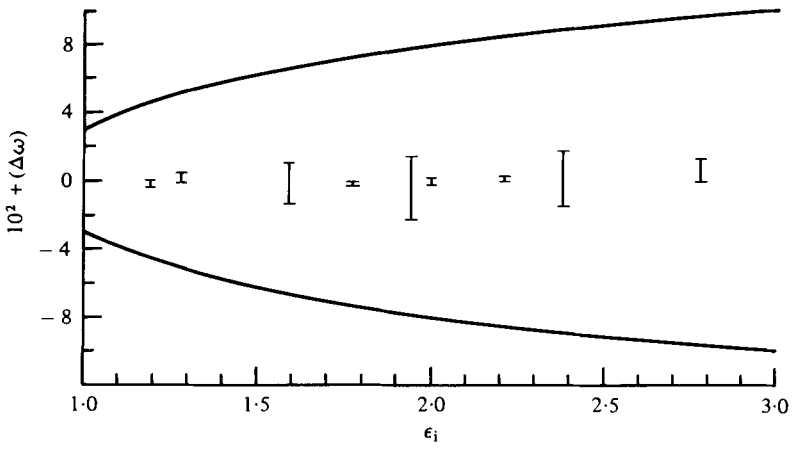

FIGURE 4. Theoretical and experimental $\Delta\omega$ for different ϵ_i. Solid curves represent the possible frequency band found from estimates as in figure 1. Vertical lines show that even within the experimental error, $\Delta\omega$ is always close to zero and never approaches the theoretical limits.

incident waves ($\epsilon_i \approx 3$), just as for normal incidence. The initial temporal growth rates of the edge waves, measured at a fixed location, agreed well with equations (8), with $\Delta\omega = 0$. For example, two peak amplitudes during the initial growth phase (but 86 s apart) had an observed ratio of 4·0 compared to a theoretical value of 4·8.

5. Discussion

Additional experiments with reflecting sidewalls showed rather bizarre edge wave behaviour. The modulation period sometimes never reached a stable value, slowly varying for hours. For cases in which a constant modulation period occurred, small changes in barrier spacing sometimes led to large changes in modulation period. Certain configurations led to a single standing subharmonic wave.

The above behaviour can be qualitatively understood by observing that the theoretical band width $\Delta\omega_{\max}$ is generally larger than the frequency splitting introduced by non-normal incidence, $\frac{1}{2}\gamma$. Typically, $\gamma = \tan\beta \sin\alpha_\infty \sim 0{\cdot}02$ while

$$\Delta\omega_{\max} > 0{\cdot}02$$

even for $\epsilon_i = 1$. Since the edge waves are standing, and must satisfy the side wall boundary conditions, the longshore wavenumbers are fixed. Thus, it will not generally be possible for the edge waves to simultaneously satisfy the resonance condition (5*a*) and the edge wave dispersion relation [equivalent to $\Delta\omega = 0$ in equation (6)]. If (5*a*) is not satisfied, the individual edge wave amplitudes and phases will never reach constant values, and neither will the apparent modulation frequency. If (5*a*) is satisfied, then $\Delta\omega$ will generally be non-zero. Since $\Delta\omega$ can be the size of $\frac{1}{2}\gamma$, a wide range of modulation frequencies, $\frac{1}{2}\gamma + \Delta\omega$, is possible. For example, if $\Delta\omega = -\frac{1}{2}\gamma$, both progressive waves are subharmonic and there is no temporal amplitude modulation. The basic conclusion is that the side wall boundary conditions, coupled with the relatively large resonant band width, make the excited edge-wave frequencies unpredictable.

Experiments with sand tracers demonstrated that migrating beach cusps were not formed by a drifting standing edge wave pattern. This is not surprising since the number of subharmonic edge-wave periods for a given antinode to drift one wavelength is γ^{-1}, in the absence of longshore currents. Observations show an even faster migration rate due to advection by currents. For these experiments $\gamma^{-1} \approx 50$, which is evidently not a long enough time for the sand tracers to respond. Even for the hypothetical case of small angle of incidence ($\alpha_\infty = 4°$) and gentle beach slope ($\beta = 2°$), $\gamma^{-1} \approx 400$, which implies that an antinodal location becomes a node every 100 subharmonic periods. Based on cusp formation times with normally incident waves, and stationary standing edge waves, this does not appear long enough to develop cusps which might conceivably migrate with the edge-wave pattern. It is rather surprising, therefore (assuming subharmonic edge waves do indeed cause beach cusps) that cusps ever form on beaches without reflective barriers at one or both ends. The requirement of almost exactly normal incidence (or symmetry about normal incidence) seems so very restrictive that it could rarely be satisfied.

6. Conclusions

Experiments with partially reflected waves, obliquely incident on a plane beach, show that the primary waves are unstable to perturbation by edge waves. The observed resonant edge-wave frequencies are close to that predicted by Guza & Bowen (1975), provided that longshore advection by mean currents resulting from partial wave breaking is taken into account. A bandwidth for possible edge-wave resonances is determined theoretically, but observations with absorbing sidewall boundaries suggest that only the edge waves with the maximum initial growth rate are excited. With reflecting sidewalls, the excited waves are scattered across the possible resonant band.

This study was supported by National Science Foundation Grant no. ENG 76-14859.

REFERENCES

GUZA, R. T. & BOWEN, A. J. 1975 The resonant instabilities of long waves obliquely incident on a beach. *J. geophys. Res.* **80**, 4529–4534.

GUZA, R. T. & BOWEN, A. J. 1976*a* Finite amplitude edge waves. *J. mar. Res.* **34**, 269–293.

GUZA, R. T. & BOWEN, A. J. 1976*b* Resonant interactions for waves breaking on a beach. *Proc. 15th Coast. Engng Conf.*, pp. 560–579.

GUZA, R. T. & DAVIS, R. E. 1974 Excitation of edge waves by waves incident on a beach. *J. geophys. Res.* **79**, 1285–1291.

GUZA, R. T. & INMAN, D. L. 1975 Edge waves and beach cusps. *J. geophys. Res.* **80**, 2997–3012.

HUNTLEY, D. A. & BOWEN, A. J. 1978 The 3-dimensional flow field on a natural beach. *Proc. 16th International Conf. on Coastal Engng* (in press).

KENYON, K. 1971 Wave refraction in ocean currents, *Deep Sea Res.* **18**, 1023–1034.

MINZONI, A. A. & WHITHAM, G. B. 1977 On the excitation of edge waves on beaches. *J. Fluid Mech.* **79**, 273–287.

ROCKLIFF, N. 1978 Finite amplitude effects in free and forced edge waves. *Math. Proc. Camb. Phil. Soc.* **83**, 463–479.